Materials Transactions, Vol. 58, No. 3 (2017) pp. 371 to 376
Special Issue on New Proposals on Titanium Production and Molten Salts

Electrolytic reduction of V_3S_4 in molten $CaCl_2$

Takahiro Matsuzaki[*1], Shungo Natsui, Tatsuya Kikuchi and Ryosuke O. Suzuki[*2]

Faculty of Engineering, Hokkaido University, Sapporo 060–8628, Japan

Metallic vanadium was successfully produced starting from vanadium sulfide by applying electrolysis in molten $CaCl_2$. Vanadium sulfide filled in a cathodic Ti basket and a graphite anode were immersed in the melt of $CaCl_2$-CaS at 1173 K in Ar, and the electrolysis was conducted at a cell voltage of 3.0 V. Sulfide electrolysis did not form carbon deposit and was free from carbon contamination, while carbon powder was formed on the cathode in the oxide electrolysis using the melt of $CaCl_2$-CaO. When the CaS content in the molten $CaCl_2$ increased, electrolysis current increased resulting in fast smelting while the oxygen and sulfur contents in metallic vanadium increased. Oxygen and sulfur contents as low as 3390 ppm and 210 ppm, respectively, were achieved by supplying about four times more electrical charge than stoichiometry.
[doi:10.2320/matertrans.M2016305]

(Received September 2, 2016; Accepted December 2, 2016; Published January 20, 2017)

Keywords: *molten salt electrolysis, vanadium sulfide, metallic vanadium, calcium chloride*

1. Introduction

Vanadium is mainly used as a solute in steel material for its high tensile strength, hardness, and fatigue resistance.[1)] Recently, vanadium has also been studied as a hydrogen storage material. Investigations of the solubility of hydrogen in vanadium and vanadium based alloys have shown that the material containing less oxygen has more hydrogen capacity than that containing more oxygen.[2)] Vanadium oxide obtained by the purification of slag from power plants is the primary feed for vanadium production. Conventionally, vanadium oxide is reduced using the aluminothermic process and purified by electron beam melting to remove impurities such as Al, Fe, and O. Since this is a batch type process, a large amount of energy is required for producing the high voltage necessary for accelerating electrons and producing an electron beam. A modified aluminothermic process was studied in the past,[3)] however, a purification process is still needed. Consequently, pure vanadium is expensive, and the operation and maintenance of the production process tends to be difficult.

Therefore, new vanadium production systems have been proposed in previous studies. In one case, Ti-V alloy as a hydrogen storage material was produced by calciothermic co-reduction of titanium oxide and vanadium oxide with molten calcium chloride.[4)] Alternatively, Miyauchi and Okabe proposed a preform reduction process for vanadium reduction[5)] that uses vapors of Mg or Ca as reductants for V_2O_5. Before reduction, the feed preform needs to be prepared by a process requiring a high temperature of 1173 K and a flux and collodion solution based binder, which consumes significant amounts of time and energy. On the other hand, Weng *et al.* produced metallic vanadium by dissolving $NaVO_3$ in a NaCl-$CaCl_2$ eutectic molten salt and electrolytically depositing vanadium.[6)]

Electrolytic reduction in molten $CaCl_2$, a process used for titanium refining, has also been applied to vanadium refining in the past.[7,8)] Oka and Suzuki investigated the reduction of vanadium by the OS (Ono Suzuki) process starting from vanadium oxide.[9)] In this process, CaO dissolved in molten $CaCl_2$ is reduced to Ca at the cathode. The Ca present near the cathode undergoes a redox reaction with V_2O_5 to produce V, while the Ca is oxidized to CaO and dissolves in the solution. Since this process is self-sustaining and supplying the reactor with metallic Ca during the process is not necessary, the process is efficient. However, significant amounts of oxygen and carbon remain in the vanadium product.

In the current study, we propose a modified OS process, in which the starting vanadium compound is vanadium sulfide instead of vanadium oxide and CaS is dissolved in molten $CaCl_2$ instead of CaO. In other words, we study a V-Ca-S reaction system. Sulfur is easier to remove from vanadium compared to oxygen, since sulfur is barely soluble in vanadium, whereas approximately 3.5 mol% of oxygen dissolves in vanadium, as indicated by vanadium-oxygen and vanadium-sulfur binary phase diagrams.[10,11)] Previously, some studies have investigated the reduction of metal sulfides such as MoS_2, Cu_2S, and $CuFeS_2$ by the electrolysis in molten salt.[12–15)] These sulfides can easily be refined by the conventional route without electrolysis. However, vanadium sulfide has a strong affinity with sulfur so that it is difficult to remove sulfur by hydrogen.

Figure 1 presents a schematic illustration of the OS process

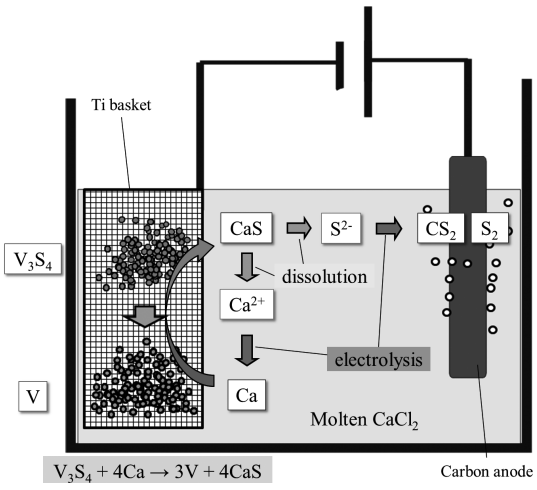

Fig. 1 Principle of the OS process starting from V_3S_4.

[*1]Graduate Student, Hokkaido University
[*2]Corresponding author, E-mail: rsuzuki@eng.hokudai.ac.jp

with vanadium sulfide as the starting material. Vanadium sulfide loaded in a Ti basket is used as the cathode. When electrolysis is conducted in a molten $CaCl_2$–CaS mixed salt solution at a voltage greater than the theoretical decomposition voltage of CaS, metallic Ca may deposit on the Ti cathode, whereas sulfur and carbon disulfide may be generated at the carbon anode.

$$2CaS \rightarrow 2Ca + S_2 \quad E^0 = 2.19V\ (1173K) \tag{1}$$

$$2CaS + C \rightarrow 2Ca + CS_2 \quad E^0 = 2.14V\ (1173K) \tag{2}$$

In this process, CaS is regenerated as the by-product of the thermic reaction and is electrolyzed repeatedly.

It is noted that V_2S_3 was registered as a chemical formula of stable sulfide in HSC database[16], however it does not appear in phase diagram of binary V-S system, where V_3S, V_5S_4, VS, VS_y, V_3S_4, V_5S_8, $V_{1+x}S_2$ and VS_4 are taken as stable phases.[11,17] Equilibrium partial pressure of sulfur at the composition of V_2S_3 at temperatures between 923 K and 1073 K is between 10^{-3} and 10^{-1} atm[18], respectively, while that in the Ca/CaS equilibrium is 10^{-42} atm[16]. It indicates that the calcium sulfurization occurs much easier than the vanadium sulfurization at V_2S_3 composition. Similarly, sulfur potentials of vanadium sulfide in the composition between VS and V_3S_4 at 1023 K through 1490 K are much higher than that of sulfurization of calcium[19]. These studies indicate calcium has sufficient ability of reduction of vanadium sulfides in various compositions.

Figure 2 describes the purification process for the feed before reduction in the conventional vanadium refining method (#1). In addition, the OS processes with vanadium oxide (#2) and vanadium sulfide (#3) as the starting material are also described. A representative raw material source for current vanadium refining plants is vanadium-containing soot obtained from power plants. In general, the slag from power plants is roasted with Na_2CO_3 to form $NaVO_3$[20], which easily dissolves in water. When $NaVO_3$ is added to an acidic solution, it dissolves selectively, leaving behind impurities in the undissolved state. NH_4VO_3 is then formed in the reaction of $NaVO_3$ with $(NH_4)_2SO_4$ in the solution.[5] NH_4VO_3 can form vanadium oxide upon calcination in open air and therefore can be utilized as the raw material for the reduction process. On the other hand, vanadium sulfide is formed via sedimentation with high pressure H_2S in the wet process.

The purpose of this study is to experimentally confirm the feasibility of the vanadium sulfide-based process and determine suitable conditions for achieving efficient electrolysis and producing high purity vanadium.

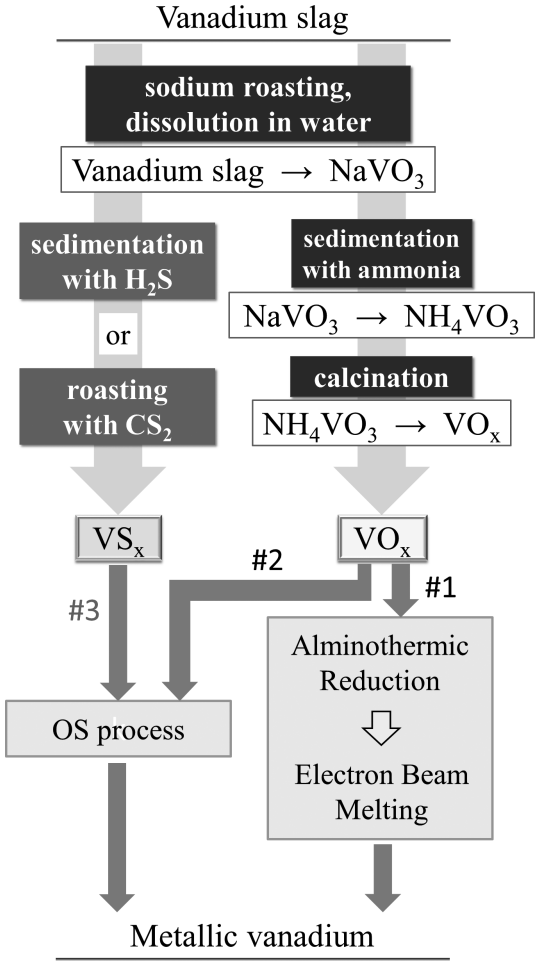

Fig. 2 Comparison of the conventional process and the process proposed in this study for the purification of the feed and production of metallic vanadium.

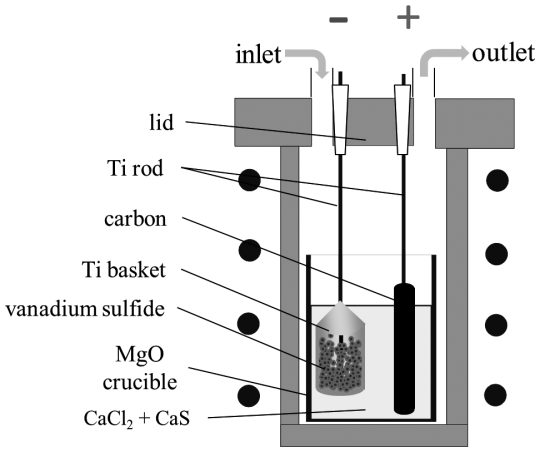

Fig. 3 Experimental setup during electrolysis.

2. Experimental Procedure

Figure 3 shows the apparatus used for vanadium reduction. Various amounts of CaS powder (300 mesh particle size, 99.99% purity, Furuuchi Chemical Co.) were added to 600 g $CaCl_2$ (95.0% purity, Wako Chemical Co.). The mixed salt was weighed and placed in a MgO crucible (90 mm in diameter, 200 mm in height) and was allowed to settle to the bottom of the chamber. A carbon rod (10 mm in diameter, 70 mm in length) attached to the tip of Ti rod (6 mm in diameter, 800 mm in length) was used as the anode. A Ti basket (12 mm in diameter, 70 mm in height, #100 mesh) attached to Ti rod was used as the cathode. The Ti basket was made of a Ti disk and Ti net (#100 mesh). A Ta wire was used for tying and stabilizing the Ti net around the Ti disk. The reagent labeled as V_2S_3 (99% purity, Furuuchi Chemical Co.) was filled in the

cathode basket. As described later, this reagent was identified as V_3S_4. The two electrodes were stabilized at the lid of the chamber. The temperature of the electrodes and mixed salt were increased at a rate of 1.67×10^{-2} K s^{-1} and maintained at 873 K for 7 h in vacuum to allow salt dehydration. Subsequently, the chamber was filled with Ar gas (99.998% purity, Air Water Co.) and constant voltage electrolysis was conducted at 3.0 V at 1173 K in the molten $CaCl_2$–CaS mixed salt electrolyte. The CaS concentration in the mixed salt was varied between 0 and 3.0 mol% while the supplied charge was constant at 2.1 of the stoichiometric reduction charge for V_3S_4 (Q_0). In another experiment, the supplied charge ratio (Q/Q_0) was varied between 1.1 and 4.3 while the CaS concentration in the melt was set at 2.0 mol%. The electrolysis for the conventional OS process starting from V_2O_3 was conducted under specific conditions. V_2O_3 is a solid at 1173 K, whereas V_2O_5 is a liquid. The electrolysis of V_2O_3 was conducted under the same conditions as those used for the reduction of V_2S_3. After electrolysis, the crucible was cooled to room temperature at a rate of 1.67×10^{-2} K s^{-1}. The cathode was recovered, washed in distilled water and acetic acid to remove the solidified salt, and then rinsed in ethanol and acetone to accelerate drying of the products. The products recovered from the salt and washing solvent were characterized by powder X-ray diffraction (XRD; Philips, X' pert pro) using Cu-K α radiation, scanning electron microscopy, oxygen and carbon analysis, and particle-size analysis.

3. Results and Discussion

In the following discussion, Q/Q_0 is the ratio of supplied charge relative to the stoichiometric reduction charge of V_3S_4 and X_{CaS} is the concentration of CaS in the mixed salt.

3.1 Morphology and phase of the samples before and after reduction

Figure 4 shows photographs of the cathode after (a) reduction and washing and (b) removal of the Ti net. After reduction, the cathode is very hard because of the salt deposits around it, and thus washing with water is necessary. The deposited product is gray in color, and the inner side of the deposit is harder than the outer side. These characteristics are observed at all electrolysis conditions.

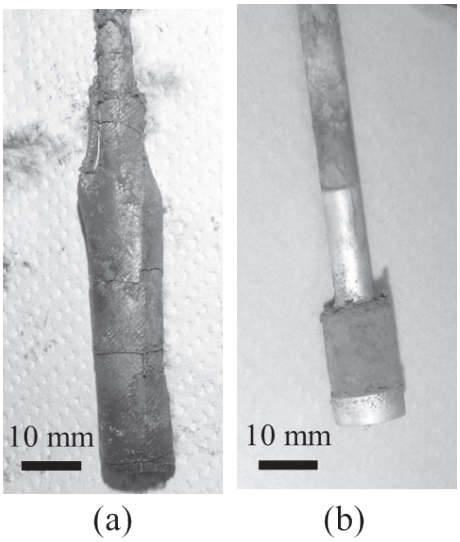

Fig. 4 Photographs of the cathode after reduction (a) before and (b) after removing the outer Ti net. (X_{CaS} = 0.5 mol%, Q/Q_0 = 2.1).

Figure 5 shows SEM images of (a) the vanadium sulfide reagent and (b) the reduced product. The starting sulfide consists of small particles of a few μm, which is agglomerated to 0.1 mm in size. The average particle diameter is determined to be 71 μm by particle-size analysis, which corresponds to agglomeration observed in the SEM image. In contrast, the reduced product is porous and exhibits a complex coral-like structure with an average particle size of 46 μm. As a result, the particle decreased in size by the reduction of sulfide, and the surface area of the samples increased. These particles sintered slightly, but they did not grow coarser during electrolysis.

Results of the XRD analysis are shown in Fig. 6. Before

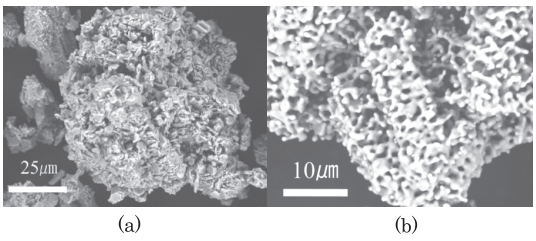

Fig. 5 SEM images of (a) the V_3S_4 reagent and (b) the product after reduction. (X_{CaS} = 2.0 mol%, Q/Q_0 = 4.3).

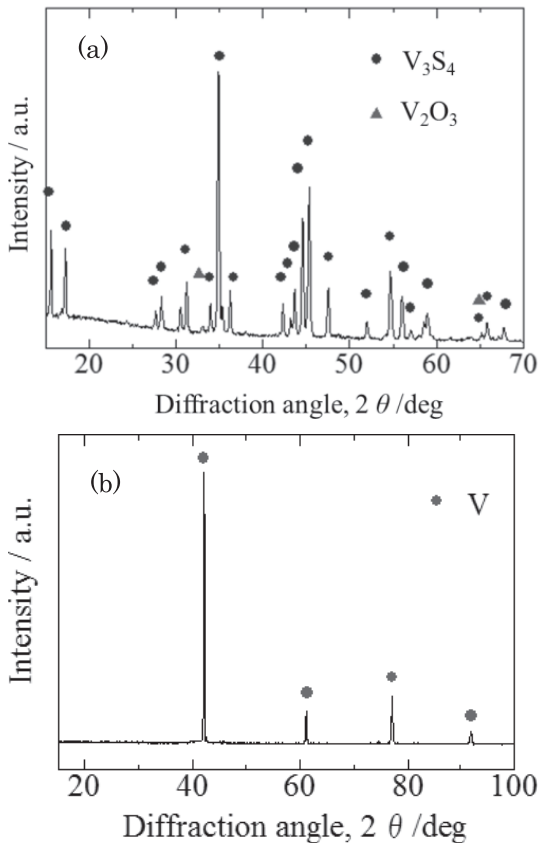

Fig. 6 XRD patterns of (a) the V_3S_4 reagent and (b) the product after reduction. (X_{CaS} = 2.0 mol%, Q/Q_0 = 4.3).

reduction, the vanadium sulfide reagent consists of the V_3S_4[21] and V_2O_3 phases. Natural desulfurization and oxidation by reaction with a small amount of oxygen might occur subsequently, so expressing this raw material as mainly V_3S_4 might be justified. However, the sulfur concentration analysis of the raw material was uncertain because concentration levels were too high for our analyzer. Judging from the XRD peak intensities, the phase ratio of V_3S_4 and V_2O_3 varied at the experimental runs. Therefore, the stoichiometric electric charge Q_0 was evaluated assuming stoichiometric V_3S_4. The product after reduction was determined to be composed of metallic vanadium, and vanadium could be smelted successfully.

3.2 Experimental confirmation of the model for the OS process with vanadium sulfide as the starting material

3.2.1 Generation of anode gaseous products at the anode

After electrolysis for 9.6 ks (Q/Q_0 = 4.3 and X_{CaS} = 2.0 mol%), a black powder was observed on the lid of the chamber, with the XRD pattern for this material shown in Fig. 7. The black powder contains solid sulfur, originating from the sulfur gas solidified on the inner surface of the cooled lid. Other impurities include titanium oxide, iron oxide, and ilmenite. The existence of Fe may be reasonably expected because the chamber is made of stainless steel, whereas Ti may have originated from the Ti rod and net used as part of the electrodes. Titanium chloride gas may also be formed by the reaction of Ti with $CaCl_2$ because of its low boiling point and its reaction with iron and oxygen.

The concentration of CS_2 in the exhaust gas during the early stages of electrolysis, as detected using a detection tube (Gastec Co.), is determined to be approximately 4 ppm (Q/Q_0 = 2.1, X_{CaS} = 0.5 mol%), a value much higher than that in ambient air.[22]

These results confirmed the generation of S_2 and CS_2 gases at the anode.

3.2.2 Electrolysis under various CaS concentration

Figure 8 shows the current-time curves measured during electrolytic reduction with various X_{CaS} values during the early stages of electrolysis. The electrolytic current decreases during the early stages of electrolysis, eventually reaching a constant value. As shown in Fig. 8, a higher X_{CaS} value in the molten salt results in enhanced electrolytic current. Although precise parameter control is needed to improve the purity of the products, the addition of a fairly large amount of CaS in molten $CaCl_2$ can shorten the electrolytic time for vanadium production. Moreover, this time-current curve indicates that the dissolution of CaS to Ca^{2+} and S^{2-} occurred and that they might be reduced and oxidized at the anode and cathode, respectively.

$$CaS \rightarrow Ca^{2+} + S^{2-} \tag{3}$$

$$Ca^{2+} + 2e^- = Ca \tag{4}$$

$$S^{2-} \rightarrow 1/2S_2 \tag{5}$$

Consequently, the deposited Ca may thermochemically react with the sulfide, as shown in Fig. 7.

$$V_3S_4 + 4Ca = 3V + 4CaS \tag{6}$$

Interestingly, metallic vanadium formed whether CaS was added or not. This result may show that a direct reduction of sulfide to metal as in reaction (7) occurs if neither CaS nor CaO perfectly dissolves in the melt.

$$V_3S_4 + 8e^- \rightarrow 3V + 4S^{2-} \tag{7}$$

The cathodic sulfide should be electroconductive if such a direct reduction occurs. As far as the authors know, the direct reduction and electrical conductivity of vanadium sulfide has not been reported.

The mechanism of metal formation should be clarified with additional electrochemical measurements, but the formation of Ca metal in the chloride salt is the most feasible explanations.

3.3 Comparison of the products of electrolytic reduction processes with vanadium oxide and vanadium sulfide as the starting materials

Figure 9 shows photographs of the upper side of the solidified salt obtained after the electrolytic reduction processes with (a) vanadium oxide and (b) vanadium sulfide as the starting materials. The values of X_{CaO} and X_{CaS} were 0.5 mol%, and the supplied charge was 2.1 for these experiments. A portion of the solidified salt after V_2O_3 reduction is black in color and appears to be composed of carbon formed from reactions (8) and (9), as indicated in previous work.[5,23]

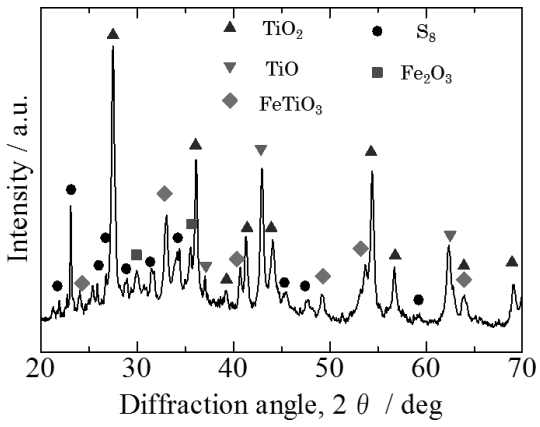

Fig. 7 XRD pattern of the black powder on the lid of the vessel.

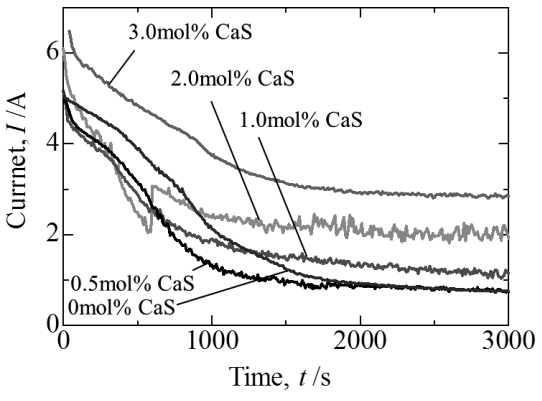

Fig. 8 Current-time curve measured during electrolysis at various X_{CaS} values.

$$CO_2 + O^{2-} \rightarrow CO_3^{2-} \quad (8)$$

$$CO_3^{2-} + 4e^- \rightarrow C + 3O^{2-} \quad (9)$$

Carbon dioxide generated from the carbon anode during electrolysis reacts with the oxide ion to form a carbonate ion. In carbonate ion rich molten salts, the reduction of carbonate ions by electrons may occur, resulting in the formation of carbon and oxide ions. As a result of this reaction, a high risk of carbon contamination in the product exists. In contrast, only $CaCl_2$ powder is observed on the upper side of the product after V_3S_4 reduction at all conditions indicating that the carbon formation does not occur in molten salt.

Figure 10 shows photographs of the cathodes after electrolytic reduction with (a) vanadium oxide and (b) vanadium sulfide as the starting materials. The Ti net after V_2O_3 reduction is brittle, whereas the Ti net after V_3S_4 reduction is ductile and retains its shape. Many of the O^{2-} ions around the cathode are supplied during the electrolytic reduction of V_2O_3, and oxygen may be absorbed by the cathode net. A strong cathode net is desirable during mass-scale production to mitigate the risk of losing products from the fracture of the cathode net.

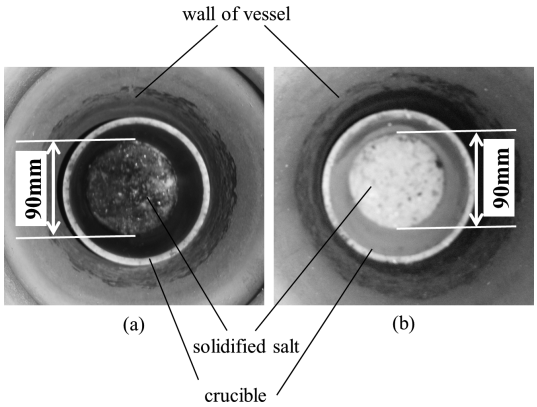

Fig. 9 Photographs of the surface of the solidified molten salt after (a) V_2O_3 and (b) V_3S_4 reduction. (X_{CaO} or X_{CaS} = 0.5 mol%, supplied charge = 2.1).

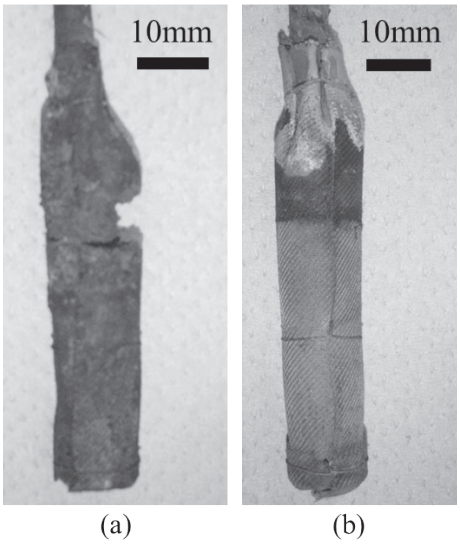

Fig. 10 Photographs of the cathode after (a) V_2O_3 and (b) V_3S_4 reduction.

3.4 Oxygen and sulfur concentrations in the samples

Figure 11 shows the relationship between X_{CaS} and oxygen/sulfur content in the vanadium product, and the average stationary current at a supplied charge (Q/Q_0) of 2.1. The average stationary current was estimated from the current-time curve shown in Fig. 8. The plot shows that an increase in the CaS content results in enhanced stationary current and a higher oxygen/sulfur content in vanadium, which may be attributed to an increase in the amount of excess Ca on the cathode. The excess Ca reacts with the gas generated at the anode and returns to CaS form, implying that the charge cannot be used for the reduction of vanadium. On the other hand, when CaS activation in the molten salt increases, the vanadium reduction reaction (6) is suppressed as per the thermodynamic equilibrium.

Similarly, Fig. 12 presents the relationship between the supplied charge and oxygen/sulfur content in vanadium when X_{CaS} is 2.0 mol%. This figure shows that with increase in the supplied charge, the oxygen and sulfur contents are reduced to 3390 ppm and 210 ppm, respectively, at a minimum. The oxygen and sulfur contents both decrease exponentially and more oxygen remains compared to sulfur. While desulfurization occurs rapidly with an increase in the supplied charge, decreasing the oxygen content in vanadium appears to be difficult. The higher oxygen content in vanadium compared to

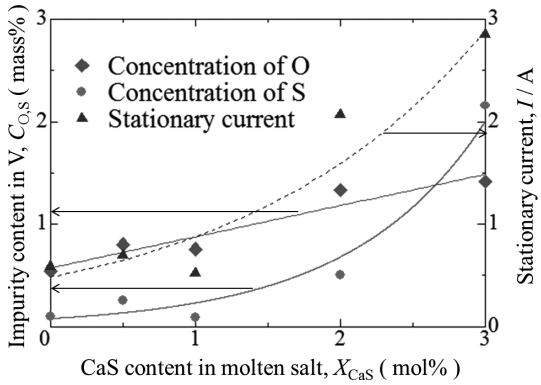

Fig. 11 Effect of CaS content in the molten salt on the oxygen and sulfur concentrations in the products and the stationary current.

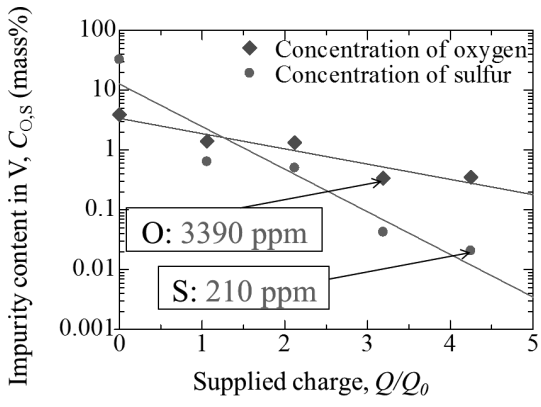

Fig. 12 Effect of supplied charge on the oxygen and sulfur concentration in the product. (The data at Q = 0 is analytical value of raw V_3S_4 reagent).

sulfur is attributed to the natural oxidation of the V_3S_4 reagent and the products, either after reduction in open air or in the washing solvent. The natural oxidation of vanadium depends on its surface area and the decrease of surface area may give a good contribution for high purity of products.

4. Conclusions

In this study, metallic vanadium was successfully produced by the OS process with vanadium sulfide as the starting material. In this process, sulfur and carbon disulfide are generated at the anode. The reduction of vanadium sulfide decreases carbon contamination and helps maintain the strength of the cathode net. When the CaS content in the mixed salt increases, the oxygen and sulfur contents in the product as well as the magnitude of the stationary current increase. On the other hand, it is possible to reduce the oxygen and sulfur contents in the product to 3000 and 200 ppm, respectively, by supplying a larger amount of charge ($Q/Q_0 = 4.3$). The products formed exhibit a large surface area, increasing the possibility of natural oxidation increases. To further enhance the purity of the refined product and the electrolysis efficiency, excluding oxygen from the products and inhibiting the desulfurization of the vanadium sulfide reagent is necessary.

Acknowledgments

The authors thank Mr. Daisuke Matsuwaka at Kobe Steel Co. Ltd. for his keen comments and discussions during this work. This study was financially supported by the Grants-in-Aid for Scientific Research (No. 25289267), by Advanced Low Carbon Technology Research and Development Program (ALCA), Japan Science and Technology Agency (JST), and by New Energy and Industrial Technology Development Organization (NEDO) under the "Innovative Structural Materials Project (Innovative Structural Materials Association (ISMA), Future Pioneering Projects).

REFERENCES

1) R.R. Moskalyk and A.M. Alfantazi: Miner. Eng. **16** (2003) 793–805.
2) M. Tsukahara, K. Takahashi, A. Isomura and T. Sakai: J. Alloy. Compd. **265** (1998) 257–263.
3) T.K. Mukherjee and C.K. Gupta: J. Less Common Met. **27** (1972) 251–254.
4) R.O. Suzuki, K. Tatemoto and H. Kitagawa: J. Alloy. Compd. **385** (2004) 173–180.
5) W. Weng, M. Wang, X. Gong, Z. Wang, D. Wang and Z. Guo: Int. J. Refract. Met. Hard Mater. **55** (2016) 47–53.
6) A. Miyauchi and T.H. Okabe: Mater. Trans. **51** (2010) 1102–1108.
7) R.O. Suzuki and S. Fukui: Mater. Trans. **45** (2004) 1665–1671.
8) H. Sakai, Y. Oka and R.O. Suzuki: J. Jpn. Inst. Met. Mater. **72** (2008) 921–927.
9) Y. Oka and R.O. Suzuki: ECS Trans. **16** (2008) 265–270.
10) H.Wriedt, Phase Diagrams of Binary Vanadium Alloys, J.F.Smith, ed., *ASM International*, Metals Park, OH (1989) pp. 175–208.
11) J.F.Smith, Phase Diagrams of Binary Vanadium Alloys, J.F.Smith, ed., *ASM International*, Metals Park, OH (1989) pp. 244–251.
12) M. Tan, R. He, Y. Yuan, Z. Wang and X. Jin: Electrochim. Acta **213** (2016) 148–154.
13) H. Gao, M. Tan, L. Rong, Z. Wang, J. Peng, X. Jin and G.Z. Chen: Phys. Chem. Chem. Phys. **16** (2014) 19514–19521.
14) T. Wang, H.P. Gao, X.B. Jin, H.L. Chen, J.J. Peng and G.Z. Chen: Electrochem. Commun. **13** (2011) 1492–1495.
15) G.Z. Chen and D.J. Fray: J. Appl. Electrochem. **31** (2001) 155–164.
16) A. Rouine, *et al.*, HSC version 6.12 (2007).
17) I. Kawada, M. Nakano-Onoda, M. Ishii and M. Saeki: J. Solid State Chem. **15** (1975) 246–252.
18) M. Wakihara, T. Uchida and M. Taniguchi: Metall. Trans. B **9** (1978) 29–32.
19) M. Nakano-Onoda and M. Nakahira: J. Solid State Chem. **30** (1979) 283–292.
20) M. Aarabi-Karasgani, F. Rashchi, N. Mostoufi and E. Vahidi: Hydrometallurgy. **102** (2010) 14–21.
21) F. Groenvold, H. Haraldsen, B. Pedersen and T. Tufte: Rev. Chim. Miner. **6** (1969) 215.
22) K. Post and R.G. Robins: Electrochim. Acta **21** (1976) 401–405.
23) K. Le Van, H. Groult, F. Lantelme, M. Dubois, D. Avignant, A. Tressaud, S. Komaba, N. Kumagai and S. Sigrist: Electrochim. Acta **54** (2009) 4566–4573.